

of the surface covered by the adsorbate. Thus, plots of  $-\ln(1 - \theta)$  versus time should be linear, with a slope proportional to the intrinsic rate of self-assembly. Figure 3 shows such a plot, for which  $\theta$  is calculated on the basis of data such as those depicted in Figure 2. As indicated, the data could be fit with a straight line (correlation factor  $r^2 = 0.99$ ) with a near-zero intercept.<sup>6</sup> The value of the intrinsic rate constant for self-assembly ( $k/[S]$ ) based on spectral areas for six independent runs at 296 K was  $(1.15 \pm 0.26) \times 10^{-2} \text{ s}^{-1} \text{ M}^{-1}$ , which compared well with that calculated on the basis of the height of the peaks,  $(0.95 \pm 0.18) \times 10^{-2} \text{ s}^{-1} \text{ M}^{-1}$ . That this value is smaller than the reported<sup>5</sup> for OTS deposition on fused silica presumably arises from reactivity differences between the oxide/hydroxide layers of silicon and germanium. However, in as much as OTS deposition provides a close-packed film with no pendant functionality influencing the deposition process, it constitutes a benchmark for understanding the self-assembly of other siloxane-anchored monolayer films.

**Acknowledgment.** Financial support from the Ohio Edison Biotechnology Center (C.N.S.) and from the Gas Research Institute (D.A.S.) is gratefully acknowledged.

(6) During its initial stages, the rate of the deposition is the largest and the signals being observed are smallest. These factors introduce a large relative uncertainty in this part of the data compared to that obtained later in the deposition process. Despite the overall goodness of fit, close inspection of the early data reveals a possible deviation from linearity, a behavior that could be ascribed to the presence of a second class of surface sites displaying much faster kinetics. More detailed studies currently underway in this laboratory are expected to shed light on this phenomenon.

## Solvent Effects on the Energetics of Prolyl Peptide Bond Isomerization

Eric S. Eberhardt, Stewart N. Loh, Andrew P. Hinck, and Ronald T. Raines\*

Department of Biochemistry  
University of Wisconsin—Madison  
Madison, Wisconsin 53706

Received March 2, 1992

The interconversion of cis (*E*) and trans (*Z*) isomers of peptide bonds that include the nitrogen of proline residues can give rise to a slow kinetic phase during protein folding.<sup>1,2</sup> This interconversion is catalyzed by the peptidyl-prolyl cis-trans isomerases (PPIases).<sup>3,4</sup> Two of these enzymes, cyclophilin and FK-506 binding protein (FKBP), have been studied extensively: (1) isotope effects<sup>5</sup> and analyses of mutant enzymes<sup>6</sup> suggest that the prolyl

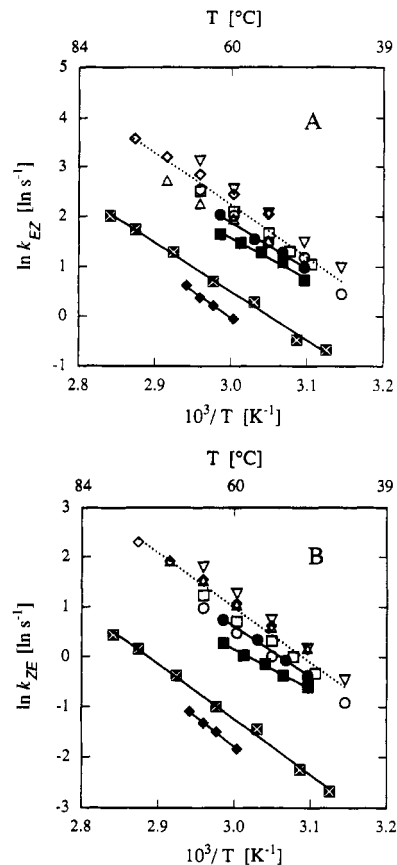


**Figure 1.** Arrhenius plots for the cis to trans (A) and trans to cis (B) isomerizations of **1** in different solvents. The solvents (dielectric constant at 25 °C) were as follows:  $\diamond$ , dioxane (2.21);  $\circ$ , benzene (2.27);  $\nabla$ , toluene (2.38);  $\bullet$ , isopropyl alcohol (19.92);  $\blacksquare$ , ethanol (24.55);  $\blacklozenge$ , trifluoroethanol (26.14);  $\square$ , acetonitrile (35.94);  $\triangle$ , *N,N*-dimethylformamide (36.71);  $\boxtimes$ , water (78.30). Linear regression analysis is shown for each protic solvent (—) and all aprotic solvents (---).

peptide bond does not suffer nucleophilic attack during catalysis, (2) calorimetry shows that binding to FKBP occurs with a large decrease in heat capacity,<sup>7</sup> and (3) structural studies of cyclophilin<sup>8</sup> and FKBP<sup>9</sup> reveal active sites composed of hydrophobic side chains.<sup>10</sup> Consequently, desolvation has been proposed as a significant contributor to catalysis by the PPIases.<sup>11</sup> This proposal is consistent with NMR line shape analyses of simple amides, which suggest that the rate of amide bond isomerization does indeed depend on solvent.<sup>12</sup> To assess the contribution of de-

\* Author to whom correspondence should be addressed.

- (1) (a) Brandts, J. F.; Halvorson, H. R.; Brennan, M. *Biochemistry* **1975**, *14*, 4953-4963. (b) Schmid, F. X.; Baldwin, R. L. *Proc. Natl. Acad. Sci. U.S.A.* **1978**, *75*, 4764-4768. (c) Kelley, R. F.; Richards, F. M. *Biochemistry* **1987**, *26*, 6765-6774. (d) Kiefhaber, T.; Quaas, R.; Hahn, U.; Schmid, F. X. *Biochemistry* **1990**, *29*, 3053-3061. (e) Hurler, M. R.; Marks, C. B.; Kosen, P. A.; Anderson, S.; Kuntz, I. D. *Biochemistry* **1990**, *29*, 4410-4419. (f) Jackson, S. E.; Fersht, A. R. *Biochemistry* **1991**, *30*, 10436-10443. (g) Kiefhaber, T.; Kohler, H.-H.; Schmid, F. X. *J. Mol. Biol.* **1992**, *224*, 217-229. (h) Kiefhaber, T.; Schmid, F. X. *J. Mol. Biol.* **1992**, *224*, 231-240.
- (2) For reviews, see: (a) Kim, P. S.; Baldwin, R. L. *Annu. Rev. Biochem.* **1982**, *51*, 459-489. (b) Nall, B. T. *Comments Mol. Cell. Biophys.* **1985**, *3*, 123-143. (c) Jaenicke, R. *Prog. Biophys. Mol. Biol.* **1987**, *49*, 117-237. (d) Kim, P. S.; Baldwin, R. L. *Annu. Rev. Biochem.* **1990**, *59*, 631-660.
- (3) (a) Fischer, G.; Bang, H.; Berger, E.; Schellenberger, A. *Biochim. Biophys. Acta* **1984**, *791*, 87-97. (b) Harrison, R. K.; Stein, R. L. *Biochemistry* **1990**, *29*, 1684-1689. (c) Harrison, R. K.; Stein, R. L. *Biochemistry* **1990**, *29*, 3813-3816. (d) Kofron, J. L.; Kuzmic, P.; Kishore, V.; Colón-Bonilla, E.; Rich, D. H. *Biochemistry* **1991**, *30*, 6127-6134, 10818.
- (4) For reviews, see: (a) Fischer, G.; Schmid, F. X. *Biochemistry* **1990**, *29*, 2205-2212. (b) Schreiber, S. L. *Science* **1991**, *251*, 283-287. (c) Gething, M.-J.; Sambrook, J. *Nature* **1992**, *355*, 33-45. (d) Cyert, M. S. *Curr. Biol.* **1992**, *2*, 18-20.
- (5) Harrison, R. K.; Caldwell, C. G.; Rosegay, A.; Melillo, D.; Stein, R. L. *J. Am. Chem. Soc.* **1990**, *112*, 7063-7064.

- (6) (a) Liu, J.; Albers, M. W.; Chen, C.-M.; Schreiber, S. L.; Walsh, C. T. *Proc. Natl. Acad. Sci. U.S.A.* **1990**, *87*, 2304-2308. (b) Park, S. T.; Aldape, R. A.; Futer, O.; DeCenzo, M. T.; Livingston, D. J. *J. Biol. Chem.* **1992**, *267*, 3316-3324.
- (7) Connelly, P. R. *Transplant. Proc.* **1991**, *23*, 2883-2885.
- (8) (a) Kallen, J.; Spitzfaden, C.; Zurini, M. G. M.; Wider, G.; Widmer, H.; Wüthrich, K.; Walkinshaw, M. D. *Nature* **1991**, *353*, 276-279. (b) Wüthrich, K.; Spitzfaden, C.; Memert, K.; Widmer, H.; Wider, G. *FEBS Lett.* **1991**, *285*, 237-247. (c) Fesik, S. W.; Gampe, R. T., Jr.; Eaton, H. L.; Gemmecker, G.; Olejniczak, E. T.; Neri, P.; Holzman, T. F.; Egan, D. A.; Edalji, R.; Simmer, R.; Helfrich, R.; Hochlowski, J.; Jackson, M. *Biochemistry* **1991**, *30*, 6574-6583. (d) Neri, P.; Meadows, R.; Gemmecker, G.; Olejniczak, E.; Nettesheim, D.; Logan, T.; Simmer, R.; Helfrich, R.; Holzman, T.; Severin, J.; Fesik, S. *FEBS Lett.* **1991**, *294*, 81-88. (e) Fesik, S. W.; Neri, P.; Meadows, R.; Olejniczak, E. T.; Gemmecker, G. *J. Am. Chem. Soc.* **1992**, *114*, 3165-3166.
- (9) (a) Moore, J. M.; Peattie, D. A.; Fitzgibbon, M. J.; Thompson, J. A. *Nature* **1991**, *351*, 248-250. (b) Michnick, S. W.; Rosen, M. K.; Wandless, T. J.; Karplus, M.; Schreiber, S. L. *Science* **1991**, *252*, 836-839. (c) Van Duyne, G. D.; Standaert, R. F.; Karplus, P. A.; Schreiber, S. L.; Clardy, J. *Science* **1991**, *252*, 839-842. (d) Van Duyne, G. D.; Standaert, R. F.; Schreiber, S. L.; Clardy, J. *J. Am. Chem. Soc.* **1991**, *113*, 7433-7434.
- (10) Stein, R. L. *Curr. Biol.* **1991**, *1*, 234-236.
- (11) (a) Radzicka, A.; Pedersen, L.; Wolfenden, R. *Biochemistry* **1988**, *27*, 4538-4541. (b) Wolfenden, R.; Radzicka, A. *Chemtracts: Biochem. Mol. Biol.* **1991**, *2* (1), 52-54.

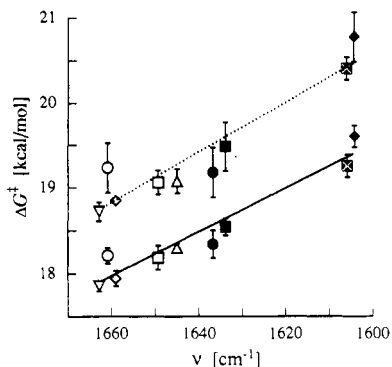
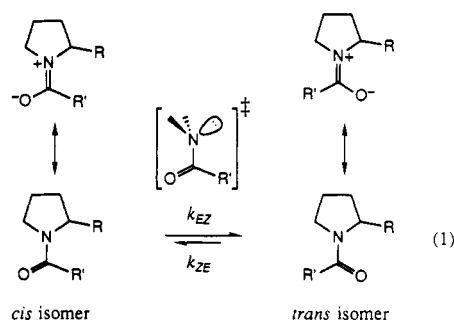


**Figure 2.** Plots of  $\Delta G^\ddagger$  for isomerization of **1** vs  $\nu$  of amide I vibrational mode of Ac-Pro-OMe in different solvents. Symbols are as in Figure 1. Values of  $\Delta G^\ddagger$  were calculated by interpolating the Arrhenius plots of Figure 1 at 60 °C. Weighted linear regression analysis is shown for cis to trans [—, slope =  $-0.025 \pm 0.003$  kcal-cm/mol] and trans to cis [---, slope =  $-0.029 \pm 0.002$  kcal-cm/mol] isomerizations.  $\Delta G^\ddagger_{\text{aprotic}} - \Delta G^\ddagger_{\text{water}} = 1.3 \pm 0.2$  kcal/mol.

solvation to catalysis by the PPIases, we have determined the effect of solvent on the energetics of prolyl peptide bond isomerization (eq 1).



We performed our analyses on the simplest dipeptide that contains a prolyl peptide bond. Racemic Ac-Gly- $[\beta, \delta\text{-}^{13}\text{C}]$ Pro-OMe (**1**) was synthesized using standard methods.<sup>13</sup> The N- and C-termini of **1** were protected so as to minimize intramolecular electrostatic interactions.<sup>14</sup> Solvent effects on the rate constants for the isomerization of the prolyl peptide bond of **1** were determined using inversion transfer <sup>13</sup>C NMR spectroscopy.<sup>15,16</sup> These measurements were performed at temperatures at which the rate constants were in the range detectable by NMR spectroscopy.<sup>17</sup> Solvent effects on the amide I vibrational mode of Ac-Pro-OMe, a model of **1** with only one amide bond, were determined using IR spectroscopy.<sup>18</sup>

(12) (a) Neuman, R. C., Jr.; Woolfenden, W. R.; Jonas, V. *J. Phys. Chem.* **1969**, *73*, 3177–3180. (b) Neuman, R. C., Jr.; Jonas, V.; Anderson, K.; Barry, R. *Biochem. Biophys. Res. Commun.* **1971**, *44*, 1156–1161. (c) Drakenberg, T.; Forsén, S. *Chem. Commun.* **1971**, 1404–1405. (d) Drakenberg, T.; Dahlqvist, K.-I.; Forsén, S. *J. Phys. Chem.* **1972**, *76*, 2178–2183.

(13) (a) Ott, D. J. *Synthesis of Stable Isotopes*; Wiley: New York, 1981; pp 34–58. (b) Young, P. E.; Torchia, D. A. In *Peptides: Structure and Function*; Hruby, V. J., Rich, D. H., Eds.; Pierce: Rockford, IL, 1983; pp 155–158. (c) Bodanszky, M. *Peptide Chemistry*; Springer-Verlag: New York, 1988; pp 66–68.

(14) (a) Evans, C. A.; Rabenstein, D. L. *J. Am. Chem. Soc.* **1974**, *96*, 7312–7317. (b) Fermanjian, S.; Tran-Dinh, S.; Savrda, J.; Sala, E.; Mermet-Bouvier, R.; Bricas, E.; Fromageot, P. *Biochim. Biophys. Acta* **1975**, *399*, 313–338.

(15) (a) Forsén, S.; Hoffman, R. A. *J. Chem. Phys.* **1963**, *39*, 2892–2901. (b) Led, J. J.; Gesmar, H. *J. Magn. Reson.* **1982**, *49*, 444–463. (c) Engler, R.; Johnston, E.; Wade, C. *J. Magn. Reson.* **1988**, *77*, 377–381.

(16) NMR experiments were done on a Bruker AM500 or Varian VXR500 instrument (125.77 MHz). Samples contained 0.1 M **1** in dry solvents that were fully deuterated (except trifluoroethanol: external deuterium lock) and neat (except water: 100 mM sodium phosphate buffer, pH 7.2, containing 80% (v/v) H<sub>2</sub>O). Isomerization rates were not altered by spiking the organic solvents with 0.2 M H<sub>2</sub>O or by halving the concentration of **1**.

(17) (a) Grathwohl, C.; Wüthrich, K. *Biopolymers* **1981**, *20*, 2623–2633. (b) Wüthrich, K. *NMR of Protein and Nucleic Acids*; Wiley: New York, 1986; pp 9,10.

The origin of the barrier to the isomerization of amide bonds is commonly attributed to the double-bond character of the C–N bond, which results in a net transfer of charge from nitrogen to the carbonyl carbon<sup>19</sup> or oxygen<sup>20</sup> (or both<sup>21</sup>). If the amide group has greater charge separation when planar than when orthogonal, then its isomerization via an orthogonal transition state should be faster in less polar solvents.<sup>22</sup> Further, if the partial charge on oxygen is greater in planar than in orthogonal amides, then protic solvents should restrict isomerization by forming a hydrogen bond to oxygen.<sup>12,23</sup>

Temperature effects on the rate constant for the isomerization of **1** in different solvents are shown as Arrhenius plots in Figure 1. The data in Figure 1 indicate qualitatively that protic solvents restrict isomerization of **1**. The rate constants for the isomerization of **1** do not, however, correlate with the solvent dielectric constant or with other measures<sup>22</sup> or solvent polarity. The rate constants do correlate with the ability of a solvent to donate a hydrogen bond. The relationship between the free energy of activation for the isomerization of **1** and the frequency of its amide I absorption band is shown in Figure 2. The amide I vibrational mode, which is primarily a C=O stretch, absorbs at lower frequencies with increasing strength of a hydrogen bond to the amide oxygen.<sup>24,25</sup> The data in Figure 2 therefore suggest that the barrier to isomerization ( $\Delta G^\ddagger$ ) is proportional to the strength of hydrogen bonds formed to the amide oxygen (given by  $\nu$ ). These results are consistent with conventional pictures of amide resonance (eq 1), which require transfer of charge between oxygen and nitrogen during isomerization.<sup>20,21</sup>

Solvent effects on the equilibrium constant for the isomerization of **1** are small. The value of the equilibrium constant for all solvents studied was  $K = k_{EZ}/k_{ZE} = 4.3 \pm 0.9$  at 60 °C, as calculated by interpolating the Arrhenius plots of Figure 1.<sup>26</sup> This lack of a solvent effect on  $K$  is also evident from the parallel lines in Figure 2. The absence of a dramatic solvent effect on  $K$  is consistent with the behavior observed for other amides.<sup>3d</sup>

Activation parameters indicate that the barrier to isomerization of **1** is almost entirely enthalpic in all solvents studied, as observed with other amides.<sup>12,27</sup> The values of  $\Delta G^\ddagger$  (Figure 2) for the isomerization of **1** are, however, 1–2 kcal/mol smaller than the analogous values for acyclic tertiary amides.<sup>12a,d</sup> The smaller barriers for prolyl peptide bond isomerization may result from pyramidalization of the prolyl nitrogen, which decreases amide resonance.<sup>28</sup>

The PPIases decrease the free energy of activation for prolyl peptide bond isomerization by 8 kcal/mol.<sup>3d</sup> Desolvation alone

(18) IR experiments were done on a Nicolet 5PC spectrometer at 25 °C using NaCl or CaF<sub>2</sub> plates or a ZnSe crystal. Samples contained 0.01 M Ac-Pro-OMe (Bachem Bioscience, Inc.), except for water and dimethylformamide, which contained 2 M Ac-Pro-OMe. The frequency of the amide I vibrational mode was determined to within 3 cm<sup>-1</sup> and was not altered by doubling the concentration of Ac-Pro-OMe or by raising the temperature to 60 °C.

(19) (a) Wiberg, K. B.; Laidig, K. E. *J. Am. Chem. Soc.* **1987**, *109*, 5935–5943. (b) Breneman, C. M.; Wiberg, K. B. *J. Comput. Chem.* **1990**, *11*, 361–373. (c) Wiberg, K. B.; Breneman, C. M. *J. Am. Chem. Soc.* **1992**, *114*, 831–840.

(20) Pauling, L. *The Nature of the Chemical Bond*, 3rd ed.; Cornell University Press: Ithaca, NY, 1960; pp 281–282.

(21) Robin, M. B.; Bovey, F. A.; Basch, H. In *The Chemistry of Amides*; Zabicky, J., Ed.; Wiley-Interscience: New York, 1970; pp 1–72.

(22) Reichardt, C. *Solvents and Solvent Effects in Organic Chemistry*; VCH: New York, 1988.

(23) Mirkin, N. G.; Krimm, S. *J. Am. Chem. Soc.* **1991**, *113*, 9742–9747.

(24) (a) Miyazawa, T.; Shimanouchi, T.; Mizushima, S. I. *J. Chem. Phys.* **1956**, *24*, 408–418. (b) Eaton, G.; Symons, M. C. R.; Rastogi, P. P. *J. Chem. Soc., Faraday Trans. 1* **1989**, *85*, 3257–3271.

(25) For reviews, see: (a) Pimentel, G. C.; McClellan, A. L. *The Hydrogen Bond*; Freeman: New York, 1960; pp 67–141. (b) Krimm, S.; Bandekar, J. *Adv. Protein Chem.* **1986**, *38*, 181–364. (c) Surewicz, W. K.; Mantsch, H. H. *Biochim. Biophys. Acta* **1988**, *952*, 115–130.

(26) The equilibrium population of the cis isomer of **1** at 60 °C varies from 14% (in trifluoroethanol) to 24% (in *N,N*-dimethylformamide).

(27) Albers, M. W.; Walsh, C. T.; Schreiber, S. L. *J. Org. Chem.* **1990**, *55*, 4984–4986.

(28) (a) Wang, Q.-P.; Bennet, A. J.; Brown, R. S.; Santarsiero, B. D. *J. Am. Chem. Soc.* **1991**, *113*, 5757–5765. (b) Bennet, A. J.; Somayaji, V.; Brown, R. S.; Santarsiero, B. D. *J. Am. Chem. Soc.* **1991**, *113*, 7563–7571.

can apparently account for 1.3 kcal/mol of this decrease (Figure 2).<sup>29</sup> Similar medium effects may modulate the stability of planar peptide bonds during the folding,<sup>1,2</sup> function,<sup>30</sup> or lysis<sup>28</sup> of proteins.

**Acknowledgment.** We thank Dave Quirk, Phil Hajduk, Dave Horita, Yijeng Liu, Kim Dirlam, and the staff at NMRFAM [Grant RR02301 (NIH)] for their assistance and Professors Sam Gellman and George Reed for helpful discussions. E.S.E. is a Wharton Predoctoral Fellow. S.N.L. is supported by Cellular and Molecular Biology Training Grant GM07215 (NIH). A.P.H. is supported by Molecular Biophysics Training Grant GM08293 (NIH). R.T.R. is a Presidential Young Investigator (NSF), Searle Scholar (Chicago Community Trust), and Shaw Scientist (Milwaukee Foundation).

**Supplementary Material Available:** Figures showing the <sup>13</sup>C NMR spectrum of **1** (CDCl<sub>3</sub>) and IR spectrum of Ac-Pro-OMe (aqueous) and a table listing activation parameters for isomerization of **1** in all solvents studied (4 pages). Ordering information is given on any current masthead page.

(29) Since the free energy of desolvation of a proline residue is 3.0 kcal/mol (Gibbs, P. R.; Radzicka, A.; Wolfenden, R. *J. Am. Chem. Soc.* **1991**, *113*, 4714–4715), desolvation destabilizes by 1.7 kcal/mol the transition state for prolyl peptide bond isomerization. Interactions (such as hydrogen bonds) may stabilize by 6.7 kcal/mol an orthogonal transition state in the active sites of the PP1ases. For a discussion of the manifestation of binding energy in enzymatic catalysis, see: Hansen, D. E.; Raines, R. T. *J. Chem. Educ.* **1990**, *67*, 483–489.

(30) (a) Dunker, A. K. *J. Theor. Biol.* **1982**, *97*, 95–127. (b) Gerwert, K.; Hess, B.; Engelhard, M. *FEBS Lett.* **1990**, *261*, 449–454. (c) Williams, K. A.; Deber, C. M. *Biochemistry* **1991**, *30*, 8919–8923.

### Correlation of Electrode Surface Structure with Activity toward H<sub>2</sub>O<sub>2</sub> Electroreduction for Bi Monolayers on Au(111)

Chun-hsien Chen and Andrew A. Gewirth\*

Department of Chemistry  
University of Illinois at Urbana–Champaign  
505 South Mathews Avenue, Urbana, Illinois 61801  
Received April 2, 1992

We present in situ atomic force microscope (AFM) images of two different structures of Bi underpotentially deposited<sup>1</sup> (upd) on Au(111). The two different structures are correlated with the activity of this surface toward the electroreduction of H<sub>2</sub>O<sub>2</sub> to H<sub>2</sub>O in acid electrolyte.

The upd of Bi on Au(111) has been well studied because the Bi overlayer acts as a catalyst for electroreduction processes.<sup>2–4</sup> The electrocatalytic activity of this surface is known to be dependent on the coverage of Bi. Three distinct stages in reactivity as a function of potential (and hence Bi coverage) have been observed.<sup>3</sup> Electrodes with intermediate coverage of Bi are significantly more active toward reduction of H<sub>2</sub>O<sub>2</sub> than either the full monolayer-covered surface or the bare Au(111). The Bi on Au system has been intensively studied, and general voltammetric response,<sup>3,5–7</sup> electroadsorption valency,<sup>8–11</sup> correlation between charge

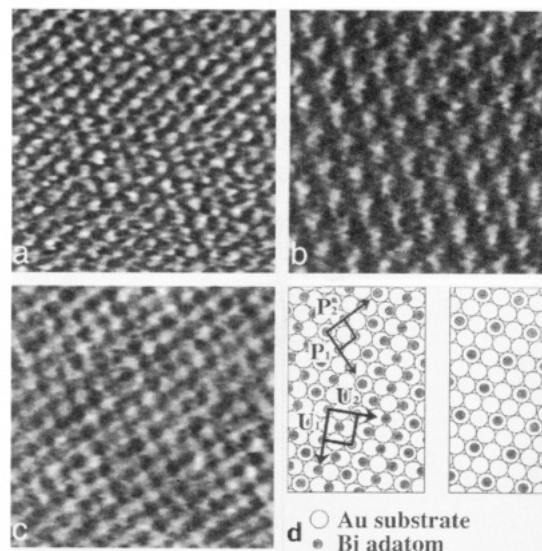


**Figure 1.** AFM images (5 × 5 nm) of Bi upd on Au(111) in 0.1 M HClO<sub>4</sub>. (a) Au(111) surface found positive of Bi upd peaks. Atom–atom distance is 0.29 nm. (b) (2 × 2)-Bi adlattice found at 200 mV vs  $E_{\text{Bi}^{3+}/0}$ . Atom–atom distance is  $0.57 \pm 0.02$  nm. (c) Uniaxially commensurate, rectangular Bi adlattice found at 100 mV. Atom–atom distance is  $0.34 \pm 0.02$  nm. (d) Schematic of Bi structures: left, rectangular lattice where P and U are primitive and nonprimitive unit cell vectors, respectively; right, (2 × 2)-Bi adlattice showing open Au and Bi sites. The Bi adatoms are larger than Au; they are shown smaller here for clarity.

and structure,<sup>12,13</sup> desorption kinetics,<sup>14,15</sup> surface conductivity,<sup>16</sup> and specular reflectivity<sup>9,17</sup> have all been examined. However, there is no direct insight available into the structures present on the surface, nor to the structural changes responsible for the changes in electrocatalytic activity. In order to understand the catalytic process, detailed in situ studies of the upd structures are necessary.

Figure 1a shows the AFM image obtained in 1 mM Bi<sup>3+</sup> + 0.1 M HClO<sub>4</sub> at potentials positive of the first Bi upd peak, which occurs at 360 mV.<sup>18</sup> This lattice exhibits a hexagonal orientation and  $0.29 \pm 0.02$  nm atom–atom spacing which corresponds to the bare Au(111) surface. When the potential is moved to between 250 and 190 mV, an overlayer of Bi atoms forms (Figure 1b). This upd overlayer is an open, hexagonal structure with an atom–atom spacing of  $0.57 \pm 0.02$  nm, which is 2 times the Au spacing. This lattice exhibits  $<5^\circ$  rotation relative to the Au lattice and is thus equivalent to a (2 × 2)-Bi commensurate structure. The right side of Figure 1d shows one arrangement of this (2 × 2)-Bi lattice; other arrangements with the Bi in 3-fold hollow or bridging sites are also possible.

(8) Schmidt, E.; Beutler, P.; Lorenz, W. *J. Ber. Bunsenges. Phys. Chem.* **1971**, *75*, 71–78.

(9) Adzic, R.; Jovancevic, V.; Podlavicky, M. *Electrochim. Acta* **1980**, *25*, 1143–1146.

(10) Deakin, M. R.; Melroy, O. *J. Electroanal. Chem.* **1988**, *239*, 321–331.

(11) Schultze, J. W. In *Proceedings of the 11 Int. Summer School on Quantum Mechanical Aspects of Electrochemistry*, Ohrid, Yugoslavia, 1972.

(12) Schultze, J. W.; Dickertmann, D. *Surf. Sci.* **1976**, *54*, 489–505.

(13) Canon, J. P.; Clavilier, J. *Surf. Sci.* **1984**, *145*, 487–518.

(14) Schultze, J. W.; Dickertmann, D. *Faraday Symp. Chem. Soc.* **1977**, *12*, 36–50.

(15) Schultze, J. W.; Dickertmann, D. *Ber. Bunsenges. Phys. Chem.* **1978**, *82*, 528–534.

(16) Romeo, F. M.; Tucceri, R. I.; Posadas, D. *Surf. Sci.* **1988**, *203*, 186–200.

(17) Takamura, K.; Watanabe, F.; Takamura, T. *Electrochim. Acta* **1981**, *26*, 979–987.

(18) Images were obtained with a NanoscopeII AFM (Digital Instruments, Santa Barbara, CA) operating with a repulsive force between tip and sample of  $10^{-9}$  N. Further experimental details are given in ref 22. AFM experiments were performed in a glove bag under an Ar atmosphere. Solutions contained 1 mM Bi<sup>3+</sup> and 0.1 M acid and were deoxygenated by Ar prior to use. The substrate was a 65 nm thick film of Au evaporated on mica, and the counter and reference electrodes were an Au wire and an Hg/Hg<sub>2</sub>SO<sub>4</sub> electrode, respectively. Potentials are reported relative to the onset of bulk Bi deposition which is  $190 \pm 5$  mV vs NHE in 0.1 M HClO<sub>4</sub>. Voltammetry was identical with the reported previously.<sup>3,14</sup>

\* To whom correspondence should be addressed.

(1) Kolb, D. M. In *Advances in Electrochemistry and Electrochemical Engineering*; Gerischer, H., Tobias, C. W., Eds.; Wiley: New York, 1978; Vol. 11, pp 125–271.

(2) Adzic, R. In *Advances in Electrochemistry and Electrochemical Engineering*; Gerischer, H., Tobias, C. W., Eds.; Wiley: New York, 1984; Vol. 13, pp 159–260.

(3) Sayed, S. M.; Juttner, K. *Electrochim. Acta* **1983**, *28*, 1635–1641.

(4) Adzic, R. R.; Markovic, N. M.; Tripkovic, A. V. *Glas. Hem. Drus. Beograd* **1980**, *45*, 399–409.

(5) Schmidt, E.; Gyax, H. R.; Cramer, Y. *Helv. Chim. Acta* **1970**, *53*, 649–654.

(6) Cadle, S. H.; Bruckenstein, S. *J. Electrochem. Soc.* **1972**, *119*, 1166–1169.

(7) Martins, M. E.; Galindo, M. C.; Arvia, A. *An. Quim.* **1990**, *86*, 327–336.